Journal of
Oral Pathology & Medicine

J Oral Pathol Med (2015) 44: 134–144

wileyonlinelibrary.com/journal/jop

doi: 10.1111/jop.12215

In situ immunohistochemical detection of intracellular *Mycoplasma salivarium* in the epithelial cells of oral leukoplakia

Harumi Mizuki, Takafumi Kawamura, Dai Nagasawa

Division of Oral and Maxillofacial Surgery, Department of Oral and Maxillofacial Reconstructive Surgery, School of Dentistry, Iwate Medical University, Morioka, Japan

BACKGROUND: Mycoplasmas are the smallest free-living organisms; *Mycoplasma salivarium* and *Mycoplasma orale* are the most common species isolated from the oropharynx. Oral leukoplakia is the most prevalent potentially malignant disorder of the oral mucosa; its etiology has not been defined. Our previous study with DNA-binding fluorescent dye suggested the presence of mycoplasmas in the epithelial cells of leukoplakia tissue.
OBJECTIVE: Our aim was to detect *M. salivarium* in the epithelial cells of leukoplakia by immunohistochemistry.
DESIGN: We produced a polyclonal antibody (PAb) reactive to *Mycoplasma* by injecting a rabbit with *M. salivarium* cells (ATCC 23064) mixed with complete Freund's adjuvant and a monoclonal antibody specific to *M. salivarium* by injecting *M. salivarium* cells (ATCC 23557) mixed with complete Freund's adjuvant into the footpads of a rat. Then, we attempted to detect *M. salivarium* in the epithelium of leukoplakia tissues by immunohistochemistry.
RESULTS: We obtained an antimycoplasma rabbit PAb reactive to all seven *Mycoplasma* species used in this study. Three hybridoma clones producing monoclonal antibodies specific to *M. salivarium* were obtained, and an *M. salivarium*-specific monoclonal antibody, designated 7-6H, was established. Immunohistochemistry with these antibodies revealed *M. salivarium* in the epithelial cells of leukoplakia with hyperplasia and hyperkeratosis on histology. PCR and sequencing verified the presence of *M. salivarium* DNA in the epithelial cells of leukoplakia.
CONCLUSION: Intracellular *M. salivarium* was identified in the epithelial cells of leukoplakia.

Correspondence: Harumi Mizuki, DDS, PhD, Division of Oral and Maxillofacial Surgery, Department of Oral and Maxillofacial Reconstructive Surgery, School of Dentistry, Iwate Medical University, 1-3-27 Chuo-dori, Morioka 020-8505, Japan. Tel: +81 19 651 5111, Fax: +81 19 651 9164, E-mail: hmizuki@iwate-med.ac.jp
Accepted for publication April 27, 2014

J Oral Pathol Med (2015) **44:** 134–144

Keywords: immunohistochemistry; intracellular location; *Mycoplasma*; oral leukoplakia

Introduction

Oral leukoplakia (OL) is the most prevalent potentially malignant disorder of the oral mucosa. OL refers to white plaques of questionable risk having excluded other known diseases or disorders that carry no increased risk of cancer (1). Histologically, the lesion is characterized as OL with or without dysplasia (1). Hyperplasia is characterized by increased cell numbers with a regularly stratified architecture and no cellular atypia. When architectural disturbance is accompanied by cytological atypia, the term dysplasia applies (2).

The etiology of OL has not been elucidated, although various etiological factors have been identified, including tobacco and alcohol use, nutritional deficiency, viral infection, and chronic irritation. Human papilloma virus (HPV) has been implicated in OL, but the role of HPV infection in this disease remains unclear (3). *Candida* has also been identified as a possible factor in the development of oral leukoplakia and malignant transformation (4).

Mizuki (5) previously reported small granular bisbenzimide-stained (Hoechst33258) fluorescent structures indicating the presence of DNA in the cytoplasm of OL epithelial cells. He concluded that the size of these structures strongly suggests the presence of microorganisms, especially bacteria. However, several observations of OL by light and electron microscopy have not revealed the presence of bacteria (6–8). We question whether these results preclude the presence of bacteria in the epithelial cells of OL.

Mycoplasmas are the smallest free-living bacteria capable of self-replication. They range in diameter from 0.2 to 0.8 μm, but unlike conventional bacteria, they lack a rigid cell wall, have a single outer membrane similar to a plasma membrane, and vary in size and shape.

Over 190 species of mycoplasma, widely distributed among humans, animals, insects, and plants, have been identified (9). Sixteen mycoplasmas have been isolated from humans (10). Several species such as *Mycoplasma pneumoniae, M. salivarium, M. orale, M. buccale, M. faucium, M. lipophilum*, and *M. fermentans* are commensals of the oropharynx (10). In the mouth, these species are isolated from gingival sulci, periodontal pockets, dental plaque, and saliva (11–13), wherein *M. salivarium* and *M. orale* are identified more frequently than the others (13, 14).

Because mycoplasmas have an extremely small genome (0.58–2.20 Mb compared with the 4.64 Mb of *Escherichia coli*), they have limited metabolic options for replication and survival (15). Thus, most mycoplasmas are thought to be parasites that remain attached to the host cell surface (16). However, several human mycoplasmas such as *Mycoplasma penetrans*, *M. pneumoniae*, *M. hominis*, *M. fermentans*, *M. genitalium*, and *M. gallisepticum* are reported to be intracellular (17–22).

Identification of mycoplasmas by light microscopy with ordinal staining such as hematoxylin–eosin is difficult, because their size is at the threshold of resolution for light microscopy. They are Gram-negative because they lack a cell wall and their membrane properties do not permit dye uptake, making staining for light microscopy impossible. Even electron microscopy cannot easily differentiate mycoplasmas from subcellular organelles without immunostaining because of the absence of a cell wall. Therefore, several specific methods are used to detect mycoplasmas, such as immunohistochemistry (IHC) and *in situ* hybridization (ISH).

Immunohistochemistry is widely used to demonstrate the existence of various substances, including microorganisms, and can be used for reliable *in situ* localization of mycoplasmas in tissue. As our preliminary study of oral leukoplakia samples by PCR indicated the presence of *M. salivarium* DNA (unpublished data), we focused on the relationship between *M. salivarium* and oral leukoplakia and attempted to detect this species in the epithelium of leukoplakia tissues by immunohistochemistry.

Materials and methods

Mycoplasma preparation

Mycoplasma salivarium (ATCC 23064, 14277, 23557, and 33130), *M. orale* (ATCC 15539), *M. buccale* (ATCC 23636), *M. fermentans* (ATCC 19989), *M. faucium* (ATCC 25293), and *Acholeplasma laidlawii* (ATCC 14192) were purchased from the American Type Culture Collection (ATCC). *M. hominis* [Gifu Type Culture Collection (GTC) 0664] was obtained from the Pathogenic Bacterial Genetic Resource Stock Center of Gifu University School of Medicine.

Pleuro-pneumonia-like organism (PPLO) medium was prepared according to the manufacturer's instructions. PPLO broth (2.1 g; Becton-Dickinson, Spark, MD, USA) was dissolved in 70 ml distilled water and sterilized by autoclaving at 121°C for 15 min. The solution was mixed with *Mycoplasma* enrichment (Becton-Dickinson) dissolved in 30 ml sterile distilled water; 50 000 U penicillin G was added aseptically.

Each strain was cultured in PPLO medium at 37°C for 5 days. For antibody production and analysis, cells were collected by centrifugation at 11 000 ***g*** for 30 min, then washed twice and resuspended with phosphate-buffered saline (PBS). The cells were fixed by incubation in 0.5% formaldehyde at 4°C for 4 days, collected by centrifugation, washed twice in PBS, and resuspended in PBS to a concentration of approximately 1 mg/ml.

Polyclonal antibody production

Whole fixed *M. salivarium* (ATCC 23064) in PBS were used as the antigen. PBS (0.25 ml) containing *M. salivarium* cells was mixed with 0.25 mg complete Freund's adjuvant (CFA) and injected into the back of a specific pathogen-free Japanese white male rabbit weighing 2.8 kg. Booster injections were administered on days 14, 28, and 42. Whole blood was collected under general anesthesia on day 52. Antiserum was purified by protein A affinity chromatography using Streamline rProtein A (Amersham Pharmacia Biotech, Buckinghamshire, UK). The purified antiserum was divided into 1-ml aliquots and stored at −80°C. Serum was taken from the same rabbit prior to immunization as a negative control.

Reactivity analysis of polyclonal antibody to M. salivarium

Fluorescent immunostaining of mycoplasma cells

Nine strains of *Mycoplasma* suspended in PBS were separately smeared as small spots on a slide and fixed with 4% formaldehyde for 15 min. After fixation, fluorescence immunostaining was performed using a biotin-free tyramide catalyzed signal amplification system (CSA II system; Dako, Carpinteria, CA, USA) according to the manufacturer's protocol; peroxidase blocking and protein blocking were omitted. The polyclonal antibody (PAb) (1:1000) diluted with an antibody diluent buffer (Antibody Diluent-Background Reducing) was applied for 30 min. Next, the slide was incubated with horseradish peroxidase (HRP)-conjugated polyclonal rabbit antibody (Rabbit Link) (1:5). After reacting with fluorescein isothiocyanate (FITC)-labeled tyramide (Amplification Reagent) for 15 min in the dark, the slide was mounted with fluorescent mounting medium and sealed with nail enamel. The slide was observed under an LSM 510 META laser microscope (Carl Zeiss, Oberkochen, Germany).

Fluorescence immunocytochemistry of Mycoplasma-infected Vero cells

Mycoplasma-infected Vero cells were prepared as follows. Vero cells (JCRB 0111) were obtained from the Japanese Collection of Research Bioresources (JCRB). The cells were cultured with advanced modified Eagle's Medium (Invitrogen, Grand Island, NY, USA) containing 5% fetal calf serum (Invitrogen) at 37°C with 5% CO_2 for 2 days. Then, 100–200 μl PPLO medium containing each of the eight *Mycoplasma* strains was added to 5 ml medium containing Vero cells and cultured for an additional 5 days. Non-infected Vero cells were prepared as negative controls. The cells were collected, suspended in PBS, and pasted onto a slide using a centrifuge (Shandon Cytospin 4; Thermo Fisher Scientific Inc., Waltham, MA, USA). *Mycoplasma* infection was confirmed by staining with DNA-binding fluorescent dye (Hoechst 33258). The slides were preserved at −80°C.

The Vero cells were fixed with 4% formaldehyde at room temperature for 10 min. After fixation, fluorescence immunocytochemistry was performed using the CSA II system according to the manufacturer's protocol. Following peroxidase and protein blocking, the cells were incubated for 1 h with the PAb (1:1000). Rabbit Link (1:5) was applied for 30 min. After treatment with Amplification Reagent for 15 min, counterstaining was performed with 4',6-Diamidino-2-phenylindole. Slides were observed by LSM 510 META laser microscopy.

Immunoelectron microscopy of Mycoplasma-infected Vero cells

Vero cells infected with *M. salivarium* were subjected to immunoelectron microscopy by ultracryotomy-immunolabeling methods, as described by Akagi et al. (23). Briefly, *M. salivarium*-infected Vero cells were collected by centrifugation and fixed with 4% paraformaldehyde in 0.1 M phosphate buffer (PB, pH 7.4) at room temperature for 2 h. The pellet was immersed in 0.1 M PB containing 30% sucrose at room temperature for 30 min and transferred to 20% polyvinylpyrrolidone and 1.84 M sucrose in 0.1 M PB at room temperature for 2 h. After infusion, the sample was frozen with liquid propane at −185°C. The frozen sample was then cut into ultrathin cryosections, and the sections were transferred to carbon-/formvar-coated grids (#100) (Nisshin EM, Tokyo, Japan). After blocking with 10% normal goat serum (Santa Cruz Biotechnology, Santa Cruz, CA, USA) in 0.1 M TBS for 1 h, the sections were incubated in 0.1 M Tris-buffered saline (TBS) containing the PAb (1:2000) at room temperature for 1 h, then at 4°C for 2 days, and finally at room temperature for 1 h. The sections were incubated for 2 h at room temperature in 0.1 M TBS containing the colloidal gold (ϕ: 10 nm)-conjugated secondary antibody (1:200) goat anti-rabbit IgG (Amersham Pharmacia Biotech). Immunolabeled sections were observed under H-7100 and H-7650 electron microscopes (Hitachi High-Technologies, Tokyo, Japan).

Monoclonal antibody production

Formaldehyde-treated *M. salivarium* (ATCC 23557) cells were used as an immunogen. First, the immunogen was emulsified with an equal volume of Freund's complete adjuvant. The emulsion (100 μl) was injected into both footpads of an 8-week-old female SD rat (SLC, Hamamatsu, Japan). Thirteen days after injection, the iliac lymph node was removed aseptically and lymphocytes were fused with P3-X63-Ag8-U1 murine myeloma cells in the presence of 50% polyethylene glycol. After fusion, the cells were suspended in RPMI 1640 containing 10% FCS and 0.1% NaN_3 and plated in 96-well culture plates.

By the third limiting dilution, 3 hybridoma clones – 2-8E, 7-6H, and 19-12D – producing monoclonal antibodies (MAbs) monospecific to *M. salivarium* were established. Three MAbs – designated MAb 2-8E, MAb 7-6H, and MAb 19-12D – produced by hybridoma clones 2-8E, 7-6H, and 19-12D, respectively, were obtained (Table 1). Their isotypes were analyzed using a rat isotyping test kit (AbD Serotec, Kidlington, UK). Finally, MAb 7-6H was chosen for its reactivity. The supernatants of hybridoma cell culture medium (RPMI 1640 containing 10% FCS) were used as an antibody.

Analysis of MAb specificity to *M. salivarium*

Western blotting was performed to analyze the cross-reactivity of MAb 7-6H to nine *Mycoplasma* strains. Membrane proteins were reacted with the MAb as the primary antibody and HRP-conjugated polyclonal rabbit anti-rat immunoglobulin as a secondary antibody.

Fluorescence immunostaining was performed as described for polyclonal antibodies. MAb 7-6H was used without dilution as the primary antibody, and HRP-conjugated polyclonal rabbit anti-rat immunoglobulin (1:100) was used as a secondary antibody. Slides were observed on an LSM 510 META laser microscope.

Immunocytochemistry of *Mycoplasma*-infected Vero cells was performed as described for the polyclonal antibodies, with some modifications. The slides were incubated with undiluted MAb for 3 h at room temperature and then for 1 h with HRP-conjugated polyclonal rabbit anti-rat immunoglobulin (1:100) as a secondary antibody. To visualize antibody–antigen interactions, the slides were

Table 1 ELISA optical density values of monoclonal antibodies (MAbs) to 8 Mycoplasma strains

	MAbs								
Species	*1-10H*	*2-8E*	*3-1B*	*3-11F*	*7-6H*	*18-1D*	*18-1G*	*19-12D*	*3-6C*
Mycoplasma hominis[a]	1.166	0.027	0.843	0.832	0.068	0.408	0.344	0.105	0.708
A. laidlawii[b]	0.744	0.101	0.735	0.602	0.069	0.741	0.724	0.102	1.119
Mycoplasma salivarium[c]	1.605	1.597	1.381	1.223	1.937	1.247	1.239	1.872	2.048
Mycoplasma orale[d]	0.668	0.057	0.640	0.683	0.098	0.482	0.469	0.137	0.711
Mycoplasma fermentans[e]	0.781	0.060	0.698	0.733	0.099	0.707	0.687	0.104	1.045
Mycoplasma buccale[f]	0.518	0.063	0.439	0.407	0.090	0.449	0.497	0.090	0.722
Mycoplasma faucium[g]	2.090	0.080	1.612	1.767	0.110	1.231	1.258	0.108	1.908
M. salivarium[h]	1.493	1.413	1.040	1.168	1.771	0.724	0.746	1.781	0.996

Each monoclonal antibody was applied to 96-well microtiter plate surfaces attached by mycoplasma cells of eight strains.
Values are optical density (OD) values at 450 nm. *Mycoplasma* strain a: *Mycoplasma hominis* (GTC 604); b: *Acholeplasma laidlawii* (ATCC 14192); c: *Mycoplasma salivarium* (ATCC 14277); d: *Mycoplasma orale* (ATCC 15539); e: *Mycoplasma fermentans* (ATCC 19989); f: *Mycoplasma buccale* (ATCC 23636); g: *Mycoplasma faucium* (ATCC 25293); h: *Mycoplasma salivarium* (ATCC 33130).

Table 2 Oral leukoplakia samples for IHC

No	*Age*	*Sex*	*Location*
1	56	M	Tongue
2	87	M	Tongue
3	72	F	Gingiva
4	70	M	Cheek
5	78	F	Gingiva
6	59	M	Tongue
7	44	M	Gingiva
8	67	M	Cheek
9	53	M	Palate
10	58	F	Lip

Table 3 Normal-appearing mucosa samples for IHC

No	*Age*	*Sex*	*Location*	*Original lesion*
1	71	M	Cheek	Hemangioma
2	26	M	Lip	Mucous cyst
3	54	M	Tongue	Fibrous hyperplasia
4	24	F	FOM	Ranula
5	46	F	Cheek	Fibrous hyperplasia
6	42	F	Cheek	Lipoma
7	79	M	Gingiva	Odontogenic tumor
8	45	F	Cheek	Fibrous hyperplasia
9	65	M	Gingiva	Bone cyst
10	21	F	Tongue	Mucous cyst

incubated with 3,3′diaminobenzidine tetrahydrochloride (DAB) solution for about 2 min with hematoxylin counterstain. The slides were observed using a light microscope.

IHC of leukoplakia

Materials for IHC and PCR analysis

Ten formalin-fixed and paraffin-embedded (FFPE) specimens of leukoplakia tissues, which were diagnosed histopathologically as hyperplasia and hyperkeratosis without invasion of *Candida*, were used for IHC (Table 2). The tissues were obtained from patients by excision for biopsy or treatment at the Department of Oral and Maxillofacial Surgery, School of Dentistry, Iwate Medical University. No invasion of *Candida* into the epithelium was confirmed by hematoxylin and eosin (H-E) staining and periodic acid-Schiff (PAS) staining. Leukoplakia tissues exhibiting hyperkeratosis or acanthosis without epithelial dysplasia were used. As a control, we used ten FFPE samples of normal-appearing oral mucosa were obtained by excision from patients with cysts, benign tumors, or other diseases for treatment (Table 3).

Unfixed oral leukoplakia tissues were used for immunoelectron microscopy or PCR analysis.

The study protocol was approved by the Ethical Committee of the School of Dentistry at Iwate Medical University (No. 1056, 1062, 1081). Informed consent was obtained from all participants.

Fluorescence IHC of leukoplakia using PAb

The specimens were cut into 4-μm serial sections and mounted on MAS-coated slides (Matsunami, Osaka, Japan). The slides were deparaffinized and rehydrated.

Fluorescence IHC was performed using PAb and the CSA II system (Dako) as described for the fluorescence immunocytochemistry of mycoplasma-infected Vero cells. In brief, after peroxidase blocking and protein blocking, slides were incubated for 3 h with the PAb (1:2000). This was followed by incubation for 1 h with peroxidase-labeled secondary antibody (1:5). Slides were observed on an LSM 510 META laser microscope. In all specimens, a portion of the serial sections was H-E stained for comparison with the fluorescent immunohistochemical stain.

IHC of leukoplakia using MAb

The specimens were cut into 4-μm serial sections and collected on MAS-coated slides. Tissue slides were deparaffinized and rehydrated. Antigen retrieval of the antigen was performed with target retrieval solution (Dako). The slides were placed in a Coplin jar filled with target retrieval solution, incubated at 95–99°C in a water bath for 20 min, and then allowed to cool for 20 min at room temperature. The slides were rinsed three times with TBST buffer.

Immunohistochemistry was performed with the CSAII system as described for immunocytochemistry of *Mycoplasma*-infected Vero cells using MAb, with modifications. Briefly, after peroxidase blocking and protein blocking, slides were incubated with undiluted MAb for 3 h at room temperature. This was followed by incubation for 1 h with HRP-conjugated polyclonal rabbit anti-rat immunoglobulin (1:100). To visualize the antibody–antigen interaction, slides were incubated with DAB solution for about 2 min and with hematoxylin counterstain, then observed by light microscopy.

As a control, IHC was performed without MAb or with normal-appearing oral mucosa samples. The findings of IHC with PAb and with MAb were compared.

Immunoelectron microscopy of leukoplakia using PAb

For immunoelectron microscopy, patient specimens were cut into pieces (0.5–1 mm^3) immediately after excision, and immunoelectron microscopy was performed using PAb, as described for immunoelectron microscopy of *Mycoplasma*-infected Vero cells. The samples were observed under H-7100 and H-7650 electron microscopes (Hitachi High-Technologies).

PCR analysis and sequencing

To reveal the localization of mycoplasmas in the leukoplakia specimens, *Mycoplasma* DNA was detected by PCR in three unfixed leukoplakia specimens. These were embedded in optimal cutting temperature (OCT) compound without prior tissue fixation, frozen rapidly, and stored at −80°C until sectioning. Cryostat sections (10-μm) were collected on aluminum membrane slides (Molecular Machines & Industries, Eching, Germany). Immunohistochemistry was performed with the CSA II system according to the manufacturer's protocol. Stained cells were removed with a laser microdissection system (Molecular Machines & Industries) and collected. These samples did not contain the surface cells of the mucosa, which could include surface-attached mycoplasmas. DNA was extracted with a DNA

Extractor WB kit (Wako, Osaka, Japan) according to the manufacturer's protocol.

Nested PCR was performed with a PCR mycoplasma detection set and *Taq* (Takara Bio Inc., Otsu, Japan) according to the manufacturer's protocol. Primers targeted the 16S and 23S rRNA genes and the spacer region between them: F1 (first forward primer, 5′-ACACCATGGGAGCT GGTAAT-3′), R1 (first reverse primer, 5′-CTTCA(T) TCGACTTT(C)CAGA-CCCAAGGCAT-3′), F2 (second forward primer, 5′-GTTCTTTGAAAACTGAAT-3′), and R2 (second reverse primer, 5′-GCATCCACCAA(T)AA(T) ACTCT-3′) (Fig. 1). PCR cycling conditions were as follows: initial denaturation for 30 s at 94°C, followed by 30 cycles of 30 s at 94°C, 2 min at 55°C, and 1 min at 72°C. The expected amplicon size from *M. salivarium* is 403 bp by the first PCR and 151 bp by the second. The first and second PCR products were electrophoresed in 1% and 3% agarose gels, respectively, and then stained with ethidium bromide and photographed on an ultraviolet transilluminator.

To identify the species of mycoplasma detected in the epithelial cells of leukoplakia tissues, we sequenced the secondary PCR products from three specimens. The second PCR products were separated by agarose gel electrophoresis and excised; three products were sequenced by the Sanger (dye terminator) method using a BigDye Terminator v3.1 cycle sequencing kit (Applied Biosystems, Foster City, CA, USA) and a 3730xl DNA analyzer (Applied Biosystems). The sequences were compared to the database of *Mycoplasma* species at the National Center for Biotechnology (NCBI)/Basic Local Alignment Search Tool (BLAST).

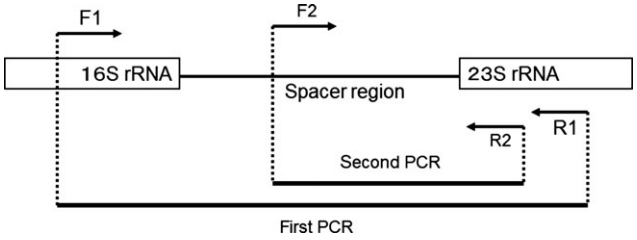

Figure 1 Nested PCR to detect *Mycoplasma* species. F1: forward primer of first PCR; R1: reverse primer of first PCR; F2: forward primer of second PCR; R2: reverse primer of second PCR.

Results

Reactivity analysis of PAb

Fluorescence immunostaining of Mycoplasma cells with PAb

Fluorescence immunostaining of *Mycoplasma* cells using the PAb showed *M. salivarium* stained as numerous fine fluorescent foci thought to represent individual *Mycoplasma* cell (Fig. 2A). The same pattern was observed with other strains. The larger fluorescent spots scattered in a field are lumps of *Mycoplasma* cells that are non-specifically stained (Fig. 2A,B).

Fluorescence IHC of Mycoplasma-infected Vero cells with PAb

Fluorescence IHC of Vero cells infected with *M. salivarium* revealed fluorescence around the cell nuclei, with no background (Fig. 3A). No fluorescence was observed in IHC without the primary antibody (control) (Fig. 3B). The antibody also reacted with other *Mycoplasma* species.

Immunoelectron microscopy of Mycoplasma-infected Vero cells with PAb

Immunoelectron microscopy showed several round electron-dense structures about 0.2–0.4 μm in diameter in the cytoplasm of Vero cells infected with *M. salivarium* (Fig. 4A,B). Some structures were present in groups (Fig. 4B). Gold particles were localized on the electron-dense structures, which were seen singly or in groups within the Vero cells (Fig. 4A,B).

Specificity analysis of MAb

Reactivity of MAbs by ELISA

Three monoclonal antibodies – MAb 2-8E, MAb 7-6H, and MAb 19-12D – were reactive to *M. salivarium* strains in ELISA (Table 1). MAb 7-6H and MAb 19-12D exhibited slightly higher density than MAbs 2-8E (Table 1). The isotypes of MAb 7-6H and MAb 19-12D were IgG2a, and MAb 2-8E was IgG2b.

Western blot analysis

Western blotting showed MAb 7-6H reacts only to *M. salivarium* (Fig. 5). The protein size of the epitope binding to MAb 7-6H was about 45 kDa (Fig. 5). The differences in band densities between the three *M. salivarium* strains are thought to be due to differences in cell number.

Fluorescence immunostaining of Mycoplasma cells with MAb

Numerous fine fluorescent foci were observed around smeared *M. salivarium* cells by fluorescent immunostaining

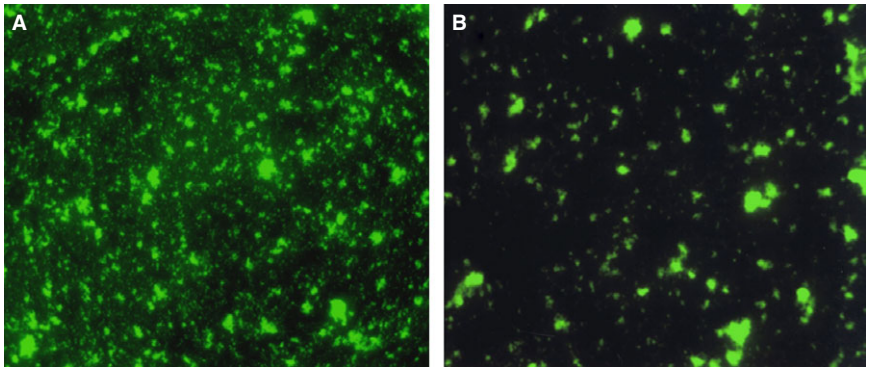

Figure 2 Fluorescence immunostaining of *Mycoplasma salivarium* cells using PAb (A). *M. salivarium* cells stained without PAb (B).

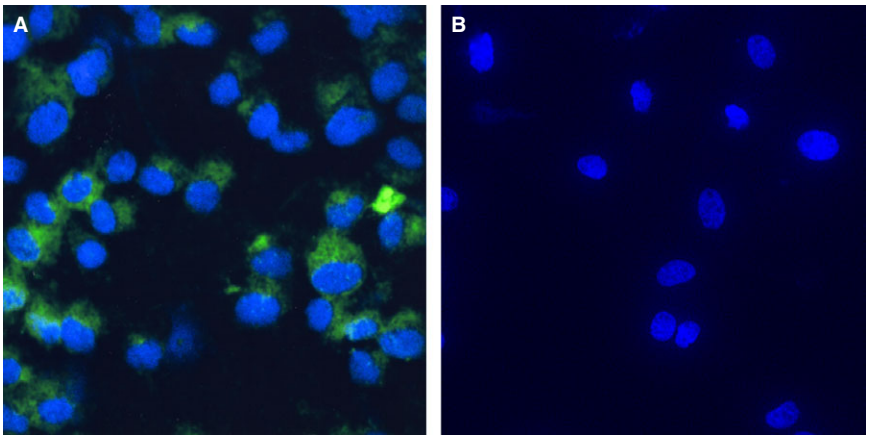

Figure 3 Fluorescence immunocytochemistry of *Mycoplasma salivarium*-infected Vero cells using PAb (A). *M. salivarium*-infected Vero cells stained without PAb (B).

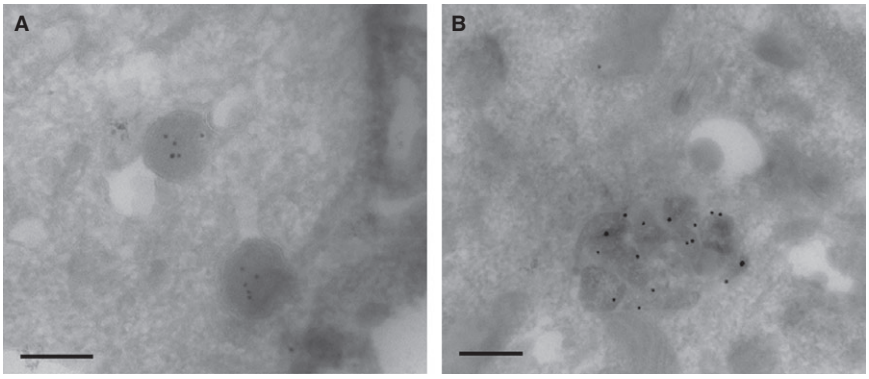

Figure 4 Immunoelectron microscopy of *Mycoplasma salivarium*-infected Vero cells. *M. salivarium* cells in the Vero cells labeled with gold particles (A, B). *M. salivarium* cells present in groups (B) (Scale bars: 0.25 μm).

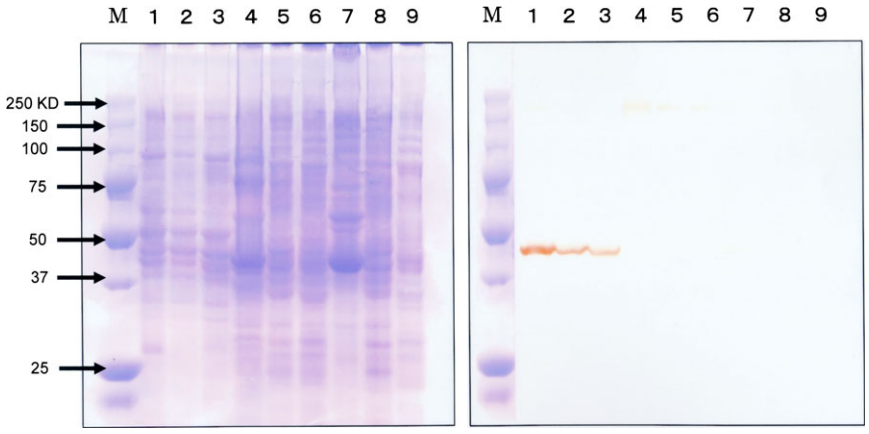

Figure 5 Western blotting of MAb 7-6H and oral *Mycoplasma* species. SDS-PAGE (left) and Western blotting (right). MAb reacted only with three *Mycoplasma salivarium* strains. Lane M: marker; Lane 1: *M. salivarium* (ATCC 14277); Lane 2: *M. salivarium* (ATCC 23557); Lane 3: *M. salivarium* (ATCC 33130); Lane 4: *Mycoplasma orale* (ATCC 15539); Lane 5: *Mycoplasma buccale* (ATCC 23636); Lane 6: *Mycoplasma faucium* (ATCC 25293); Lane 7: *Mycoplasma hominis* (GTC 664); Lane 8: *Mycoplasma fermentans* (ATCC 19989); Lane 9: *Acholeplasma laidlawii* (ATCC 14192).

using MAb 7-6H, as they were with the PAb (Fig. 6A). However, these fluorescent dots were not observed with *M. orale* (Fig. 6B) or other *Mycoplasma* species. Immunostaining without MAb 7-6H yielded no fine fluorescent dots.

Immunocytochemistry of Mycoplasma-infected Vero cells using MAb

Vero cells infected with *M. salivarium* exhibited fine granular staining around the nuclei; there was no staining in the background (Fig. 7A). No clearly positive reactions were observed around Vero cells infected with *M. orale*

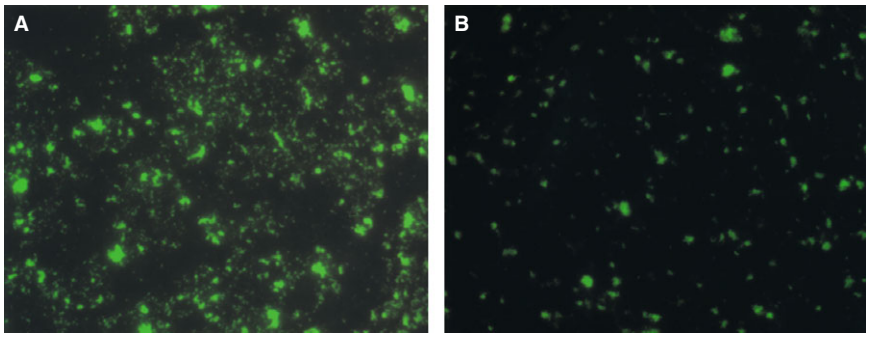

Figure 6 Fluorescence immunostaining of *Mycoplasma salivarium* cells (A) and *Mycoplasma orale* cells (B) using MAb.

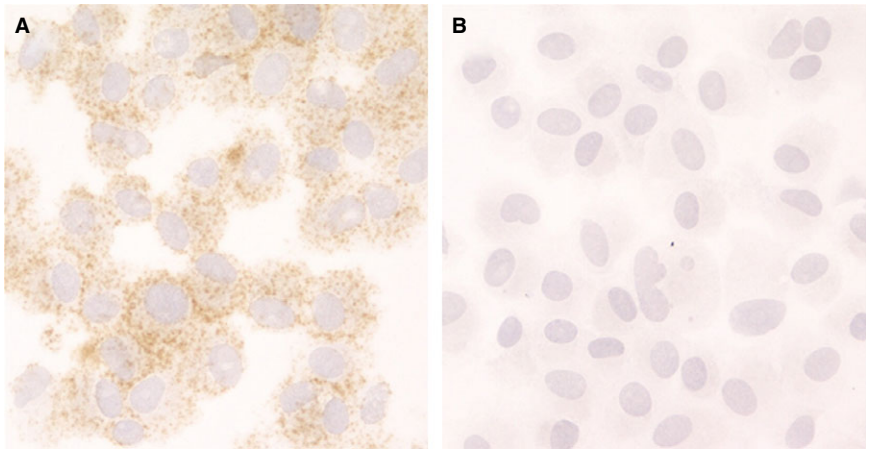

Figure 7 Immunocytochemistry of Vero cells infected with *Mycoplasma salivarium* (A) and *Mycoplasma orale* (B) using MAb.

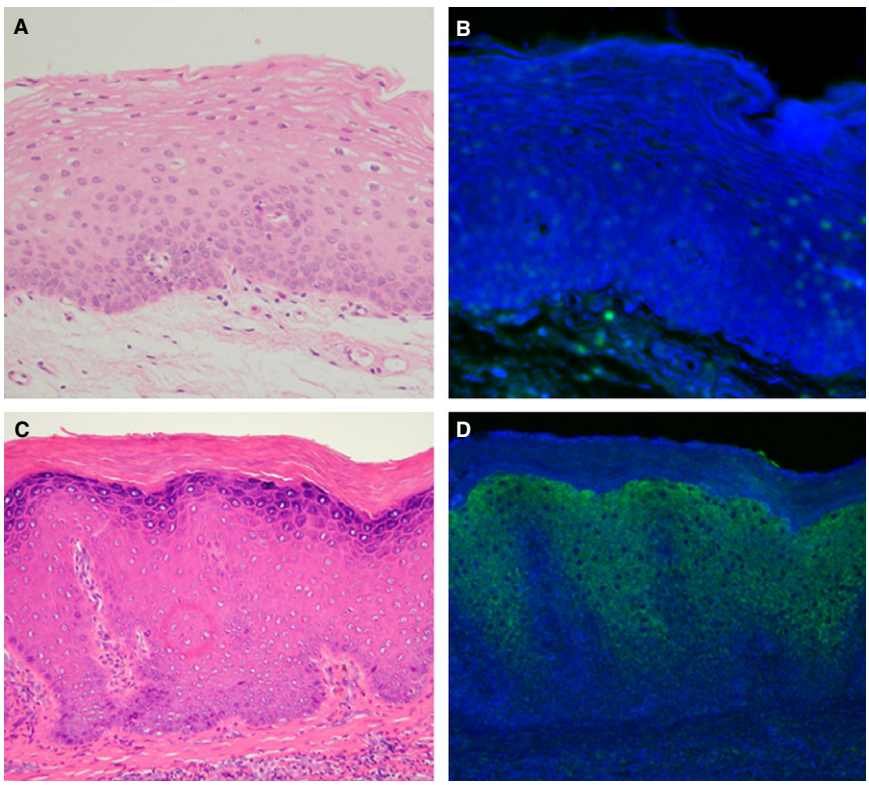

Figure 8 HE staining (A) and fluorescence immunohistochemistry (IHC) using PAb (B) of normal-appearing mucosa. HE staining (C) and fluorescence IHC (D) of a leukoplakia specimen.

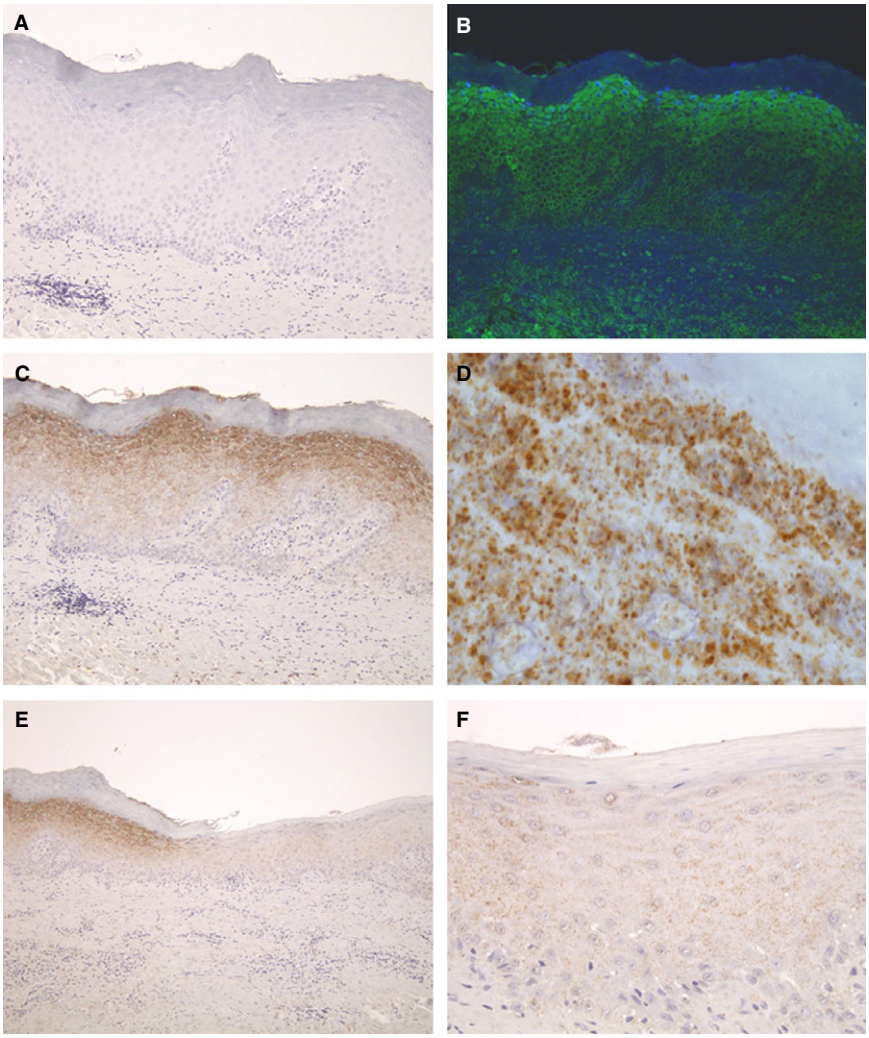

Figure 9 Immunohistochemistry (IHC) of similar areas of sections of a leukoplakia specimen (A–C): IHC without MAb (A), fluorescence IHC using PAb (B), and IHC using MAb (C). A high-magnification image of positive reactions (D); an area showing both positive and weak reactions (E); a high-magnification image of the weak reactions shown in E (F).

(Fig. 7B), or other strains. Immunocytochemistry without the MAb showed no positive staining.

IHC of leukoplakia

Fluorescence IHC using PAb

Fluorescence IHC of leukoplakia tissues revealed bright green fluorescence in or between the epithelial cells (Fig. 8D). All ten samples yielded positive reactions. In contrast, normal-appearing mucosa showed little to no fluorescence in the epithelial layer (Fig. 8B). Fluorescence was uniform, not granular, and was brighter in granular and prickle cells than in the basal cells (Fig. 8D). Little to no fluorescence was observed in the orthokeratotic layers. In a few specimens, fluorescence was seen in the lamina propria, which we conclude is non-specific staining.

IHC using MAb

All ten OL specimens showed positive reactions as brown stains in the epithelial layer by IHC using MAb (Fig. 9C). The amount of stain varied between specimens or regions in a section. More staining was observed in granular and prickle cells than in basal cells (Fig. 9C). Little to no stain was seen in the orthokeratotic layers, and no staining was observed in the lamina propria (Fig. 9C,E).

In comparisons, areas of positive MAb stain were consistent with those obtained with PAb (Fig. 9B,C), although the areas stained with PAb were wider. This is thought to be due to the different sensitivities of the PAb and MAb. No staining was observed in IHC performed without MAb (Fig. 9A). Positive reactions were observed as numerous fine brown granules in the epithelial cells of leukoplakia tissues (Fig. 9D). In one section, both strongly stained and slightly stained areas were observed (Fig. 9E), possibly indicating high MAb specificity. The surface of strongly stained area showed hyperorthokeratosis, while that of the slightly stained area was less keratinized.

Immunoelectron microscopy of leukoplakia tissue with PAb

Immunoelectron microscopy revealed the presence of numerous electron-dense structures within the cytoplasm

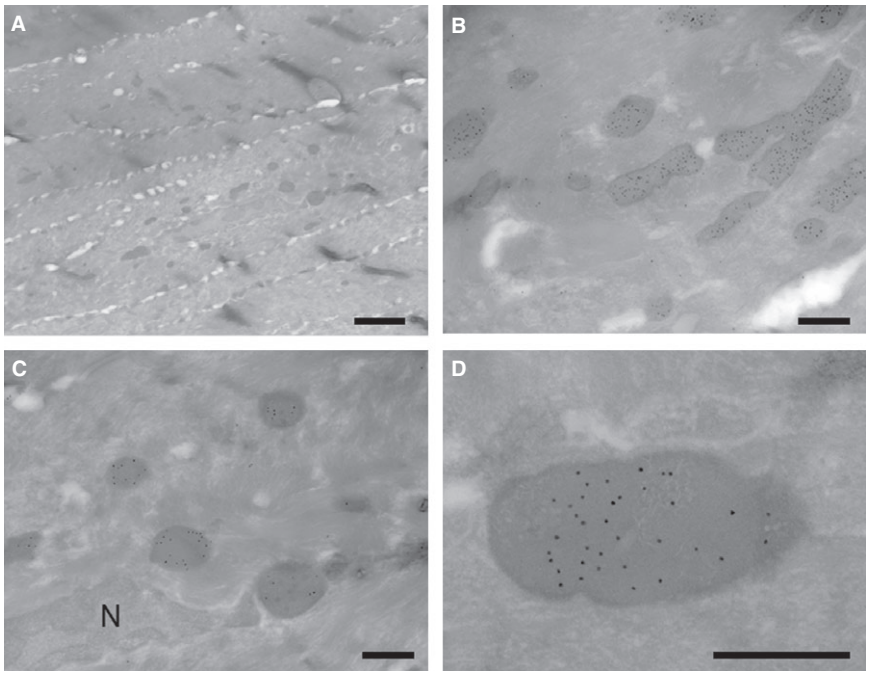

Figure 10 Immunoelectron microscopy of oral leukoplakia specimens using PAb: (A) scale bar; 2 μm. (B) scale bar; 0.5 μm. (C) N; nucleus, scale bar; 0.5 μm. A high-magnification image of a structure (D) scale bar; 0.5 μm.

of epithelial cells of leukoplakia tissues (Fig. 10A–C). Most of these structures were observed in cells from the granular cell layer to the spinosal cell layer. They were polymorphous and varied in size and had homogeneous inner structures with high electron density. The density was almost the same among them (Fig. 10A–C). They were appeared to lack a rigid cell wall and had definite borders (Fig. 10D). Binding of gold particles was observed on the electron-dense structures (Fig. 10B–D). These structures were observed less frequently, if at all, within normal oral epithelial cells, which was consistent with the fluorescence immunohistochemistry results.

PCR and sequencing of PCR products

Nested PCR indicated the presence of *Mycoplasmas* DNA in the DNA extracted from the epithelial cells of leukoplakia tissue in three samples. The second PCR produced a fragment of about 150 bp, similar to *M. salivarium*.

Sequence analysis indicated the length of the second PCR products was 151 bp, and their sequences were the same in all three samples. Sequence similarity searching using NCBI/BLAST indicated 100% similarity to *M. salivarium*.

Discussion

We detected *M. salivarium* in the epithelial cells of OL tissues by IHC. This is the first report of intracellular localization of *M. salivarium* in the epithelial cells of human oral mucosa.

Before IHC, we produced a PAb and a MAb reactive to *M. salivarium*. The rabbit PAb was reactive to *M. salivarium* and others of the six tested *Mycoplasma* species. Its reactivity to mycoplasmas was demonstrated by immunoelectron microscopy. In contrast, the MAb exhibited specificity only to *M. salivarium*. In addition, the PAb and MAb were applicable for IHC in FFPE specimens.

Although Blazek et al. (24) developed MAbs specific to *A. laidlawii*, *M. hyorhinis*, *M. orale*, *M. arginini,* or *M. salivarium* and the MAb CCM-2 reactive to all five *Mycoplasma* species, the specificity of these MAbs was not analyzed with the exception of MAb CCM-2. Therefore, we assert that our MAb is the first antibody with demonstrated specificity for *M. salivarium*.

Immunohistochemistry techniques are usually used for *in situ* detection of microorganisms including mycoplasmas. It offers numerous advantages in the diagnosis and study of mycoplasma infections. It also allows simultaneous visualization of mycoplasma and its cellular or tissue localization, enabling detailed pathogenesis studies. Because of its sensitivity and versatility, the ABC method is the most commonly used immunohistochemical method. In particular, highly sensitive methods such as ABC are required for FFPE tissue sections. Lo et al. (25) revealed *M. fermentans* cells in the lung and liver of patients with respiratory distress syndrome using the ABC method and *M. fermentans*-specific MAb. We initially tried to detect mycoplasmas in the cells of OL using the ABC method, but we were not successful, for unknown reasons.

We chose the CSA II system, a biotin-free tyramide catalyzed signal amplification system to detect *M. salivarium* in FFPE sections of leukoplakia tissue. The CSA II system is a supersensitive IHC method that is an improved version of the catalyzed signal amplification method (CSA method) (26) and can amplify signal densities approximately 100 times better than the ABC method (27). Therefore, this method is suitable for visualizing mycoplasmas. On the other hand, it has the disadvantage of increased background staining. Nevertheless, our MAb

showed high sensitivity and specificity, but little background staining.

The CSA II system has two mechanisms for visualizing an antibody–antigen interaction: fluorescence staining and DAB staining. In this study, fluorescence staining was applied to IHC with PAb to reduce background. DAB staining was used for IHC with MAb for clear, high-contrast imaging.

Positive staining was observed in epithelial cells by IHC using the PAb and MAb. The results were similar, except the width of the stained areas was greater with the PAb than with the MAb, possibly due to their different sensitivities.

Immunoelectron microscopy revealed gold-labeled structures in the cytoplasm of epithelial cells. Further, the structures were perinuclear and thus at a distance from the cell membrane. Therefore, we conclude that *M. salivarium* is intracellularly localized.

The presence of *M. salivarium* in the epithelium of OL was also confirmed by PCR amplification using DNA extracted from OL samples and sequencing.

Most mycoplasmas are thought to be surface parasites. However, intracellular localization of an *M. penetrans* strain isolated from the urogenital tract of a patient with acquired immunodeficiency syndrome (AIDS) was reported in HeLa cells (17). In addition, *M. pneumoniae* (18), *M. hominis* (19), *M. fermentans* (20), *M. genitalium* (21), and *M. gallisepticum* (22) reside within non-phagocytic cells such as HeLa cells, Vero cells, human spermatozoa, and human lung carcinoma cell lines under certain circumstances. Most of their intracellular localization was investigated by cell culture. Our study showed *in vivo* localization of *M. salivarium* cells in the cytoplasm of epithelial cells. Further, they were bound by a single membrane and maintained their structures in the cytoplasm of epithelial cells on immunoelectron microscopy, which may suggest their survival. Intracellular survival and multiplication of mycoplasmas has been reported by several papers (15).

Mycoplasma contamination has many effects on host cells in culture, including induction of cytokine expression or chromosomal aberrations (28). Although the *in vivo* expression of cytokines on OL tissue has not been clarified, increased expression of salivary interleukin 6 and tumor necrosis factor alpha in patients with OL has been reported (29). However, the relation between cytokine production and leukoplakia has not been elucidated. It is now clear that prolonged interactions between mammalian cells and mycoplasmas could induce chromosomal instability and malignant transformation (30–32). This might be related to malignant transformation of leukoplakia, but it has not been clear.

We limited our study to OL with hyperplasia and hyperkeratosis. All samples showed the presence of *M. salivarium* in the epithelial cells. Further, the areas of OL with a thick cornified layer showed strong positive reactions, while less positive staining was seen in areas with a thin cornified layer. These findings may suggest the intracellular localization of *M. salivarium* is related to hyperplasia and hyperkeratosis of oral mucosa.

We believe there is a relationship between *M. salivarium* infection and the development of OL, but the pathogenesis of *M. salivarium* infections *in vivo* remains unclear. As hyperplasia is considered the initial stage prior to dysplasia in the multistep process of cancer development (33), *M. salivarium* infection into the oral mucosa may be a factor at the onset of OL. This demonstration of intracellular localization of *M. salivarium* in leukoplakia tissues advances our understanding of the etiology of OL.

In conclusion, we detected immunohistochemically intracellular *M. salivarium* in the epithelial cells of oral leukoplakia using PAb reactive to *Mycoplasma* species and MAb specific to *M. salivarium*.

References

1. Warnakulasuriya S, Johson NW, Van Der Waal I. Nomenclature and classification of potentially malignant disorders of the oral mucosa. *J Oral Pathol Med* 2007; **36**: 575–80.
2. Warnakulasuriya S, Reibel J, Bouquo J, Dabelsteen E. Oral epithelial dysplasia classification systems: predictive value, utility, weaknesses and scope for improvement. *J Oral Pathol Med* 2008; **37**: 127–33.
3. Saghravanian N, Ghazvini K, Babakoohi S, Firooz A, Mohtasham N. Low prevalence of high risk genotypes of human papilloma virus in abnormal oral mucosa, oral leukoplakia and verrucous carcinoma. *Acta Odontol Scand* 2011; **69**: 406–9.
4. Sharma P, Saxena S. *Candida albicans* and its correlation with oral epithelial neoplasia. *Int J Oral-Med Sci* 2011; **10**: 140–8.
5. Mizuki H. *In situ* staining with DNA-binding fluorescent dye, Hoechst 33258, to detect microorganisms in epithelial cells of oral leukoplakia. *Oral Oncol* 2001; **37**: 521–6.
6. Hashimoto K, Richard J, Dibella RJ, Tarnowski WM, Shklar G. Electron microscopic studies of oral leukoplakia. *Oral Surg* 1068; **25**: 901–13.
7. Banoczy J, Juhasz J, Albrecht M. Ultrastructure of different clinical forms of oral leukoplakia. *J Oral Pathol* 1980; **9**: 41–53.
8. Kannan S, Balaram P, Pillai MR, et al. Ultrastructural variations and assessment of malignant transformation risk in oral leukoplakia. *Pathol Res Pract* 1993; **189**: 1169–80.
9. Rottem S, Naot Y. Subversion and exploitation of host cells by mycoplasmas. *Trends Microbiol* 1998; **6**: 436–40.
10. Blanchard A, Bebear CM. Mycoplasmas of humans. In: Razin S, Herrmann R, eds. *Molecular biology and pathogenicity of mycoplasmas*. New York: Kluwer Academic/Plenum Publishers, 2002; 45–71.
11. Kumagai K, Iwabuchi T, Hinuma Y, Yuki K, Ishida N. Incidence, species, and significance of mycoplasma species in the mouth. *J Infect Dis* 1971; **123**: 16–21.
12. Uchida A. Isolation and enumeration of mycoplasmas in dental plaques. *Bull Tokyo Med Dent Univ* 1981; **28**: 117–23.
13. Watanabe T, Matsuura M, Seto K. Enumeration, isolation, and species identification of mycoplasma in saliva sampled from the normal and pathological human oral cavity and antibody response to an oral mycoplasma (*Mycoplasma salivarium*). *J Clin Microbiol* 1986; **23**: 1034–8.
14. Engel LD, Kenny GE. *Mycoplasma salivarium* in human gingival sulci. *J Periodontal Res* 1970; **5**: 163–70.
15. Rottem S. Interaction of mycoplasmas with host cells. *Physiol Rev* 2002; **83**: 417–32.
16. Razin S, Yogev D, Naot Y. Molecular biology and pathogenicity of mycoplasmas. *Microbiol Rev* 1998; **63**: 1094–156.
17. Tarshis M, Yavlovich A, Katzenell A, Ginsburg I, Rottem S. Intracellular location and survival of *Mycoplasma penetrans* within HeLa cells. *Curr Microbiol* 2004; **49**: 136–40.
18. Yavlovich A, Tarshis M, Rottem S. Internalization and intracellular survival of *Mycoplasma pneumoniae* by non-phagocytic cells. *FEMS Microbiol Lett* 2004; **233**: 241–6.

19. Diaz-Garcia FJ, Herrera-Mendoza AP, Giono-Cerezo S, Guerra-Infante FM. *Mycoplasma hominis* attaches to and locates intracellularly in human spermatozoa. *Hum Reprod* 2006; **21**: 1591–8.
20. Yavlovich A, Katzenell A, Tarshis M, Higazi AA-H, Rottem S. *Mycoplasma fermentans* binds to and invades HeLa cells: involvement of plasminogen and urokinase. *Infect Immun* 2004; **72**: 5004–11.
21. Jensen JS, Blom J, Lind K. Intracellular location of *Mycoplasma genitalium* in cultured Vero cells as demonstrated by electron microscopy. *Int J Exp Pathol* 1994; **75**: 91–8.
22. Winner F, Rosengarten R, Citti C. In vitro cell invasion of *Mycoplasma gallisepticum*. *Infect Immun* 2000; **68**: 4238–44.
23. Akagi T, Ishida K, Hanasaka T, et al. Improved methods for ultracryotomy of CNS tissue for ultrastructural and immunogold analysis. *J Neurosci Methods* 2006; **153**: 276–82.
24. Blazek R, Schmitt K, Krafft U, Hadding U. Fast and simple procedure for the detection of cell culture mycoplasmas using a single monoclonal antibody. *J Immunol Methods* 1990; **131**: 203–12.
25. Lo SC, Wear DJ, Green SL, Jones PG, Legier JF. Adult respiratory distress syndrome with or without systemic disease associated with infections due to *Mycoplasma fermentans*. *Clin Infect Dis* 1993; **17**(Suppl 1): 259–63.
26. Kunze E, Middel P, Fayyzi A, Schweyer S. Immunohistochemical staining of plastic (methyl-methacrylate)–embedded bone marrow biopsies applying the biotin-free tyramide signal amplification system. *Appl Immunohistochem Mol Morphol* 2008; **16**: 76–82.
27. Sanno A, Osamura RT. Catalyzed reporter deposition method for amplifying endocrine products. *Endocr Pathol* 1998; **9**: 195–9.
28. Drexler HG, Uphoff CC. Mycoplasma contamination of cell cultures: incidence, source, effects, detection, elimination, prevention. *Cytotechnology* 2002; **39**: 75–90.
29. Brailo V, Vucicevic-Boras V, Cekic-Arambasin A, Alajberg IZ, Milenovic A, Lukac J. The significance of salivary interleukin 6 and tumor necrosis factor alpha in patients with leukoplakia. *Oral Oncol* 2006; **42**: 370–3.
30. Feng SH, Tsam S, Rodriguez J, Lo SC. Mycoplasma infections prevent apoptosis and induce malignant transformation of interleukin-3-dependent 32D hematopoietic cells. *Mol Cell Biol* 1999; **19**: 7995–8002.
31. Tsai S, Wear DJ, Shih JW, Lo SC. Mycoplasma and oncogenesis persistent infection and multistage malignant transformation. *Proc Natl Acad Sci U S A* 1995; **92**: 10197–201.
32. Zhang B, Shih JW, Wear DJ, Tsai S, Lo SC. High-level expression of H-ras and c-myc oncogenes in mycoplasma-mediated malignant cell transformation. *Proc Soc Exp Biol Med* 1997; **214**: 359–66.
33. Mao L. Leukoplakia: molecular understanding of pre-malignant lesions and implications for clinical management. *Mol Med Today* 1997; **3**: 442–8.

Acknowledgements

We thank Prof. Koujiro Tohyama and Mr. Kinji Ishida of the Center for Electron Microscopy and Bio-Imaging Research, Central Research Laboratories for their help with immunoelectron microscopy by ultracryotomy-immunolabeling methods. This work was supported in part by Grants-in Aid for High-Tech Research Project (2005-2009) from the Ministry of Education, Culture, Sports, Science, and Technology of Japan.